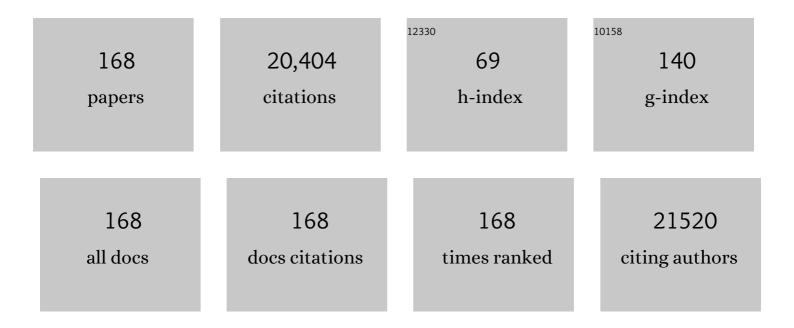
Omid Oakhavan

List of Publications by Year in descending order

Source: https://exaly.com/author-pdf/1453145/publications.pdf Version: 2024-02-01



ΟΜΙΟ ΟΛΚΗΛΊΛΛΝ

#	Article	IF	CITATIONS
1	Electrically conductive carbonâ€based (bio)â€nanomaterials for cardiac tissue engineering. Bioengineering and Translational Medicine, 2023, 8, .	7.1	29
2	Green products from herbal medicine wastes by subcritical water treatment. Journal of Hazardous Materials, 2022, 424, 127294.	12.4	26
3	Green porous benzamide-like nanomembranes for hazardous cations detection, separation, and concentration adjustment. Journal of Hazardous Materials, 2022, 423, 127130.	12.4	34
4	Green metal-organic frameworks (MOFs) for biomedical applications. Microporous and Mesoporous Materials, 2022, 335, 111670.	4.4	65
5	Aperiodic perforated graphene in optical nanocavity absorbers. Materials Science and Engineering B: Solid-State Materials for Advanced Technology, 2022, 276, 115557.	3.5	7
6	Strain effects on optical properties of linearly polarized resonant modes in the presence of monolayer graphene. Materials Science and Engineering B: Solid-State Materials for Advanced Technology, 2022, 277, 115584.	3.5	6
7	Silver and Gold Nanoparticles for Antimicrobial Purposes against Multi-Drug Resistance Bacteria. Materials, 2022, 15, 1799.	2.9	58
8	Graphene nanopores in broadband wide-angle optical cavity resonance absorbers. Surfaces and Interfaces, 2022, 30, 101956.	3.0	8
9	Graphene-based Nanomaterials in Fighting the Most Challenging Viruses and Immunogenic Disorders. ACS Biomaterials Science and Engineering, 2022, 8, 54-81.	5.2	29
10	Reduced polydopamine coated graphene for delivery of Hset1 antisense as A photothermal and gene therapy of breast cancer. Journal of Drug Delivery Science and Technology, 2022, 73, 103462.	3.0	6
11	Nanomaterials for Photocatalytic Degradations of Analgesic, Mucolytic and Anti-Biotic/Viral/Inflammatory Drugs Widely Used in Controlling SARS-CoV-2. Catalysts, 2022, 12, 667.	3.5	36
12	Metal-organic frameworks (MOF) based heat transfer: A comprehensive review. Chemical Engineering Journal, 2022, 449, 137700.	12.7	39
13	CaZnO-based nanoghosts for the detection of ssDNA, pCRISPR and recombinant SARS-CoV-2 spike antigen and targeted delivery of doxorubicin. Chemosphere, 2022, 306, 135578.	8.2	28
14	Viral infected cells reveal distinct polarization behavior; a polarimetric microscopy analysis on HSV infected Vero and HeLa cells. Journal of Quantitative Spectroscopy and Radiative Transfer, 2021, 262, 107484.	2.3	1
15	All-Carbon Negative Differential Resistance Nanodevice Using a Single Flake of Nanoporous Graphene. ACS Applied Electronic Materials, 2021, 3, 3418-3427.	4.3	22
16	Prevascularized Micro-/Nano-Sized Spheroid/Bead Aggregates for Vascular Tissue Engineering. Nano-Micro Letters, 2021, 13, 182.	27.0	33
17	Synthesis, morpho-structural properties, and catalytic performances of Pt-APA@Fe3O4/GO nanocomposite based on magnetical graphene in C–C coupling reactions and photoinactivation of E. coli. Journal of Nanoparticle Research, 2021, 23, 1.	1.9	5
18	Pressure-engineered electrophoretic deposition for gentamicin loading within osteoblast-specific cellulose nanofiber scaffolds. Materials Chemistry and Physics, 2021, 272, 125018.	4.0	42

#	Article	IF	CITATIONS
19	Review of Oxygenation with Nanobubbles: Possible Treatment for Hypoxic COVID-19 Patients. ACS Applied Nano Materials, 2021, 4, 11386-11412.	5.0	28
20	Single-Layer MoS2-MoO3-x Heterojunction Nanosheets with Simultaneous Photoluminescence and Co-Photocatalytic Features. Catalysts, 2021, 11, 1445.	3.5	30
21	Emerging Phospholipid Nanobiomaterials for Biomedical Applications to Lab-on-a-Chip, Drug Delivery, and Cellular Engineering. ACS Applied Bio Materials, 2021, 4, 8110-8128.	4.6	17
22	Graphene aerogel nanoparticles for in-situ loading/pH sensitive releasing anticancer drugs. Colloids and Surfaces B: Biointerfaces, 2020, 186, 110712.	5.0	52
23	Graphene/CuO ₂ Nanoshuttles with Controllable Release of Oxygen Nanobubbles Promoting Interruption of Bacterial Respiration. ACS Applied Materials & Interfaces, 2020, 12, 35813-35825.	8.0	124
24	<p>Graphene Oxide Negatively Regulates Cell Cycle in Embryonic Fibroblast Cells</p> . International Journal of Nanomedicine, 2020, Volume 15, 6201-6209.	6.7	19
25	Graphene Oxide Papers in Nanogenerators for Self-Powered Humidity Sensing by Finger Tapping. Scientific Reports, 2020, 10, 7312.	3.3	63
26	Ultrahigh Permeable C ₂ N-Inspired Graphene Nanomesh Membranes versus Highly Strained C ₂ N for Reverse Osmosis Desalination. Journal of Physical Chemistry B, 2019, 123, 8740-8752.	2.6	22
27	Selenium nanoparticles for targeted stroke therapy through modulation of inflammatory and metabolic signaling. Scientific Reports, 2019, 9, 6044.	3.3	208
28	Three-Dimensional Graphene Foams: Synthesis, Properties, Biocompatibility, Biodegradability, and Applications in Tissue Engineering. ACS Biomaterials Science and Engineering, 2019, 5, 193-214.	5.2	121
29	The bio-interface between functionalized Au NR@GO nanoplatforms with protein corona and their impact on delivery and release system. Colloids and Surfaces B: Biointerfaces, 2019, 173, 891-898.	5.0	30
30	Curcumin as a green fluorescent label to revive the fluorescence property of functionalized graphene oxide nanosheets. Journal of Drug Delivery Science and Technology, 2018, 45, 422-427.	3.0	15
31	Supercritical water in top-down formation of tunable-sized graphene quantum dots applicable in effective photothermal treatments of tissues. Carbon, 2018, 130, 267-272.	10.3	75
32	Photoluminescence and electrochemical investigation of curcumin-reduced graphene oxide sheets. Journal of the Iranian Chemical Society, 2018, 15, 351-357.	2.2	10
33	Cationic graphene oxide nanoplatform mediates miR-101 delivery to promote apoptosis by regulating autophagy and stress. International Journal of Nanomedicine, 2018, Volume 13, 5865-5886.	6.7	29
34	Graphene oxide in generation of nanobubbles using controllable microvortices of jet flows. Carbon, 2018, 138, 8-17.	10.3	38
35	Toxicity and Safety Issues of Carbon Nanotubes. , 2018, , 145-171.		11
36	Multifunctional core-shell nanoplatforms (gold@graphene oxide) with mediated NIR thermal therapy to promote miRNA delivery. Nanomedicine: Nanotechnology, Biology, and Medicine, 2018, 14, 1891-1903.	3.3	54

#	Article	IF	CITATIONS
37	Novel synthesis of cobalt/poly vinyl alcohol/gamma alumina nanocomposite for catalytic application. Applied Physics A: Materials Science and Processing, 2017, 123, 1.	2.3	17
38	Nanoscale graphene oxide sheets as highly efficient carbocatalysts in green oxidation of benzylic alcohols and aromatic aldehydes. Chinese Journal of Catalysis, 2017, 38, 745-757.	14.0	20
39	Highly sensitive selective sensing of nickel ions using repeatable fluorescence quenching-emerging of the CdTe quantum dots. Materials Research Bulletin, 2017, 95, 532-538.	5.2	35
40	Antioxidant nanomaterials in advanced diagnoses and treatments of ischemia reperfusion injuries. Journal of Materials Chemistry B, 2017, 5, 9452-9476.	5.8	169
41	Apoptotic and anti-apoptotic genes transcripts patterns of graphene in mice. Materials Science and Engineering C, 2017, 71, 460-464.	7.3	9
42	Role of cooling rate in selective synthesis of graphene and carbon nanotube on Fe foil using hot filament chemical vapor deposition. , 2016, , .		1
43	Improving the photocatalytic activity of graphene oxide/ZnO nanorod films by UV irradiation. Applied Surface Science, 2016, 371, 590-595.	6.1	180
44	Synthesis and cyto-genotoxicity evaluation of graphene on mice spermatogonial stem cells. Colloids and Surfaces B: Biointerfaces, 2016, 146, 770-776.	5.0	50
45	Graphene Jet Nanomotors in Remote Controllable Self-Propulsion Swimmers in Pure Water. Nano Letters, 2016, 16, 5619-5630.	9.1	60
46	Toward Chemical Perfection of Graphene-Based Gene Carrier via Ugi Multicomponent Assembly Process. Biomacromolecules, 2016, 17, 2963-2971.	5.4	45
47	Influence of heavy nanocrystals on spermatozoa and fertility of mammals. Materials Science and Engineering C, 2016, 69, 52-59.	7.3	57
48	Graphene oxide for rapid determination of testosterone in the presence of cetyltrimethylammonium bromide in urine and blood plasma of athletes. Materials Science and Engineering C, 2016, 61, 246-250.	7.3	22
49	Ugi Four-Component Assembly Process: An Efficient Approach for One-Pot Multifunctionalization of Nanographene Oxide in Water and Its Application in Lipase Immobilization. Chemistry of Materials, 2016, 28, 3004-3016.	6.7	63
50	Graphene scaffolds in progressive nanotechnology/stem cell-based tissue engineering of the nervous system. Journal of Materials Chemistry B, 2016, 4, 3169-3190.	5.8	174
51	Solid state preparation and photocatalytic activity of bismuth oxybromide nanoplates. Research on Chemical Intermediates, 2016, 42, 2429-2447.	2.7	19
52	Mechanochemically prepared BiOCl nanoplates for removal of rhodamine B and pentachlorophenol. Monatshefte Für Chemie, 2016, 147, 685-696.	1.8	15
53	Rolled graphene oxide foams as three-dimensional scaffolds for growth of neural fibers using electrical stimulation of stem cells. Carbon, 2016, 97, 71-77.	10.3	200
54	Curcumin-reduced graphene oxide sheets and their effects on human breast cancer cells. Materials Science and Engineering C, 2015, 55, 482-489.	7.3	122

#	Article	IF	CITATIONS
55	Magnetite/dextran-functionalized graphene oxide nanosheets for in vivo positive contrast magnetic resonance imaging. RSC Advances, 2015, 5, 47529-47537.	3.6	37
56	Photocatalytic activity of CuO nanoparticles incorporated in mesoporous structure prepared from bis(2-aminonicotinato) copper(II) microflakes. Transactions of Nonferrous Metals Society of China, 2015, 25, 3634-3642.	4.2	57
57	Near infrared laser stimulation of human neural stem cells into neurons on graphene nanomesh semiconductors. Colloids and Surfaces B: Biointerfaces, 2015, 126, 313-321.	5.0	98
58	Hydrothermally Synthesized CuO Powders for Photocatalytic Inactivation of Bacteria. Acta Physica Polonica A, 2015, 127, 1727-1731.	0.5	17
59	Microwave-assisted synthesis of bismuth oxybromochloride nanoflakes for visible light photodegradation of pollutants. Physica B: Condensed Matter, 2015, 475, 14-20.	2.7	22
60	Personalized disease-specific protein corona influences the therapeutic impact of graphene oxide. Nanoscale, 2015, 7, 8978-8994.	5.6	199
61	High-efficiency CdTe/CdS core/shell nanocrystals in water enabled by photo-induced colloidal hetero-epitaxy of CdS shelling at room temperature. Nano Research, 2015, 8, 2317-2328.	10.4	38
62	Hydrogen-rich water for green reduction of graphene oxide suspensions. International Journal of Hydrogen Energy, 2015, 40, 5553-5560.	7.1	37
63	Photocatalytic activity of mesoporous microbricks of ZnO nanoparticles prepared by the thermal decomposition of bis(2-aminonicotinato) zinc (II). Chinese Journal of Catalysis, 2015, 36, 742-749.	14.0	25
64	Visible light photoinactivation of bacteria by tungsten oxide nanostructures formed on a tungsten foil. Applied Surface Science, 2015, 338, 55-60.	6.1	35
65	Dose-dependent effects of nanoscale graphene oxide on reproduction capability of mammals. Carbon, 2015, 95, 309-317.	10.3	122
66	ZnFe2O4 nanoparticles as radiosensitizers in radiotherapy of human prostate cancer cells. Materials Science and Engineering C, 2015, 46, 394-399.	7.3	97
67	Bacteriorhodopsin as a superior substitute for hydrazine in chemical reduction of single-layer graphene oxide sheets. Carbon, 2015, 81, 158-166.	10.3	283
68	Accelerated differentiation of neural stem cells into neurons on ginseng-reduced graphene oxide sheets. Carbon, 2014, 66, 395-406.	10.3	215
69	Superparamagnetic zinc ferrite spinel–graphene nanostructures for fast wastewater purification. Carbon, 2014, 69, 230-238.	10.3	208
70	Flexible bactericidal graphene oxide–chitosan layers for stem cell proliferation. Applied Surface Science, 2014, 301, 456-462.	6.1	126
71	Zinc ferrite spinel-graphene in magneto-photothermal therapy of cancer. Journal of Materials Chemistry B, 2014, 2, 3306.	5.8	128
72	Pulsed laser irradiation for environment friendly reduction of graphene oxide suspensions. Applied Surface Science, 2014, 301, 183-188.	6.1	79

OMID OAKHAVAN

#	Article	IF	CITATIONS
73	Pd–WO3/reduced graphene oxide hierarchical nanostructures as efficient hydrogen gas sensors. International Journal of Hydrogen Energy, 2014, 39, 8169-8179.	7.1	163
74	Synthesis of graphene from natural and industrial carbonaceous wastes. RSC Advances, 2014, 4, 20441.	3.6	189
75	Vertically aligned ZnO@CdS nanorod heterostructures for visible light photoinactivation of bacteria. Journal of Alloys and Compounds, 2014, 590, 507-513.	5.5	72
76	Hyperthermia-induced protein corona improves the therapeutic effects of zinc ferrite spinel-graphene sheets against cancer. RSC Advances, 2014, 4, 62557-62565.	3.6	50
77	DNA and RNA extractions from eukaryotic and prokaryotic cells by graphene nanoplatelets. RSC Advances, 2014, 4, 60720-60728.	3.6	39
78	In vivo SPECT imaging of tumors by 198,199Au-labeled graphene oxide nanostructures. Materials Science and Engineering C, 2014, 45, 196-204.	7.3	116
79	The use of graphene in the self-organized differentiation of human neural stem cells into neurons under pulsed laser stimulation. Journal of Materials Chemistry B, 2014, 2, 5602.	5.8	99
80	Spongy graphene electrode in electrochemical detection of leukemia at single-cell levels. Carbon, 2014, 79, 654-663.	10.3	105
81	Cyto and genotoxicities of graphene oxide and reduced graphene oxide sheets on spermatozoa. RSC Advances, 2014, 4, 27213.	3.6	117
82	Ultra-sensitive detection of leukemia by graphene. Nanoscale, 2014, 6, 14810-14819.	5.6	106
83	Cytotoxicity of protein corona-graphene oxide nanoribbons on human epithelial cells. Applied Surface Science, 2014, 320, 596-601.	6.1	51
84	Graphene oxide sheets involved in vertically aligned zinc oxide nanowires for visible light photoinactivation of bacteria. Journal of Alloys and Compounds, 2014, 612, 380-385.	5.5	74
85	Polyphenols attached graphene nanosheets for high efficiency NIR mediated photodestruction of cancer cells. Materials Science and Engineering C, 2013, 33, 1498-1505.	7.3	64
86	Flash photo stimulation of human neural stem cells on graphene/TiO2 heterojunction for differentiation into neurons. Nanoscale, 2013, 5, 10316.	5.6	203
87	DNA-decorated graphene nanomesh for detection of chemical vapors. Applied Physics Letters, 2013, 103, 183110.	3.3	45
88	Graphene: Promises, Facts, Opportunities, and Challenges in Nanomedicine. Chemical Reviews, 2013, 113, 3407-3424.	47.7	643
89	Genotoxicity of graphene nanoribbons in human mesenchymal stem cells. Carbon, 2013, 54, 419-431.	10.3	239
90	Visible light-induced photocatalytic reduction of graphene oxide by tungsten oxide thin films. Applied Surface Science, 2013, 276, 628-634.	6.1	26

#	Article	IF	CITATIONS
91	Graphene nanogrids for selective and fast osteogenic differentiation of human mesenchymal stem cells. Carbon, 2013, 59, 200-211.	10.3	215
92	Graphene Nanomesh Promises Extremely Efficient In Vivo Photothermal Therapy. Small, 2013, 9, 3593-3601.	10.0	348
93	Differentiation of human neural stem cells into neural networks on graphene nanogrids. Journal of Materials Chemistry B, 2013, 1, 6291.	5.8	153
94	Nontoxic concentrations of PEGylated graphene nanoribbons for selective cancer cell imaging and photothermal therapy. Journal of Materials Chemistry, 2012, 22, 20626.	6.7	195
95	Adverse effects of graphene incorporated in TiO2 photocatalyst on minuscule animals under solar light irradiation. Journal of Materials Chemistry, 2012, 22, 23260.	6.7	147
96	Toward Single-DNA Electrochemical Biosensing by Graphene Nanowalls. ACS Nano, 2012, 6, 2904-2916.	14.6	438
97	The decoration of TiO2/reduced graphene oxide by Pd and Pt nanoparticles for hydrogen gas sensing. International Journal of Hydrogen Energy, 2012, 37, 15423-15432.	7.1	130
98	Size-dependent genotoxicity of graphene nanoplatelets in human stem cells. Biomaterials, 2012, 33, 8017-8025.	11.4	662
99	Graphene oxide strongly inhibits amyloid beta fibrillation. Nanoscale, 2012, 4, 7322.	5.6	197
100	Protein Degradation and RNA Efflux of Viruses Photocatalyzed by Graphene–Tungsten Oxide Composite Under Visible Light Irradiation. Journal of Physical Chemistry C, 2012, 116, 9653-9659.	3.1	287
101	The use of a glucose-reduced graphene oxide suspension for photothermal cancer therapy. Journal of Materials Chemistry, 2012, 22, 13773.	6.7	393
102	Escherichia coli bacteria reduce graphene oxide to bactericidal graphene in a self-limiting manner. Carbon, 2012, 50, 1853-1860.	10.3	497
103	Increasing the antioxidant activity of green tea polyphenols in the presence of iron for the reduction of graphene oxide. Carbon, 2012, 50, 3015-3025.	10.3	240
104	Silver nanoparticles within vertically aligned multi-wall carbon nanotubes with open tips for antibacterial purposes. Journal of Materials Chemistry, 2011, 21, 387-393.	6.7	142
105	Copper oxide nanoflakes as highly sensitive and fast response self-sterilizing biosensors. Journal of Materials Chemistry, 2011, 21, 12935.	6.7	115
106	Melatonin as a powerful bio-antioxidant for reduction of graphene oxide. Journal of Materials Chemistry, 2011, 21, 10907.	6.7	255
107	CuO/Cu(OH)2 hierarchical nanostructures as bactericidal photocatalysts. Journal of Materials Chemistry, 2011, 21, 9634.	6.7	260
108	Wrapping Bacteria by Graphene Nanosheets for Isolation from Environment, Reactivation by Sonication, and Inactivation by Near-Infrared Irradiation. Journal of Physical Chemistry B, 2011, 115, 6279-6288.	2.6	578

#	Article	IF	CITATIONS
109	Functionalized carbon nanotubes in ZnO thin films for photoinactivation of bacteria. Materials Chemistry and Physics, 2011, 130, 598-602.	4.0	115
110	Photocatalytic reduction of graphene oxides hybridized by ZnO nanoparticles in ethanol. Carbon, 2011, 49, 11-18.	10.3	355
111	The effect of heat treatment on physical properties of nanograined (WO3)1–x–(Fe2O3)x thin films. Vacuum, 2011, 85, 810-819.	3.5	21
112	AFM Spectral Analysis of Self–Agglomerated Metallic Nanoparticles on Silica Thin Films. Current Nanoscience, 2010, 6, 116-123.	1.2	7
113	Toxicity of Graphene and Graphene Oxide Nanowalls Against Bacteria. ACS Nano, 2010, 4, 5731-5736.	14.6	2,223
114	Graphene Nanomesh by ZnO Nanorod Photocatalysts. ACS Nano, 2010, 4, 4174-4180.	14.6	675
115	Thickness dependent activity of nanostructured TiO2/α-Fe2O3 photocatalyst thin films. Applied Surface Science, 2010, 257, 1724-1728.	6.1	114
116	Improved electrochromical properties of sol–gel WO3 thin films by doping gold nanocrystals. Thin Solid Films, 2010, 518, 2250-2257.	1.8	81
117	Self-accumulated Ag nanoparticles on mesoporous TiO2 thin film with high bactericidal activities. Surface and Coatings Technology, 2010, 204, 3676-3683.	4.8	157
118	Cu and CuO nanoparticles immobilized by silica thin films as antibacterial materials and photocatalysts. Surface and Coatings Technology, 2010, 205, 219-223.	4.8	218
119	Mechano-chemical AFM nanolithography of metallic thin films: A statistical analysis. Current Applied Physics, 2010, 10, 1203-1210.	2.4	3
120	The effect of heat treatment on formation of graphene thin films from graphene oxide nanosheets. Carbon, 2010, 48, 509-519.	10.3	507
121	Photodegradation of Graphene Oxide Sheets by TiO ₂ Nanoparticles after a Photocatalytic Reduction. Journal of Physical Chemistry C, 2010, 114, 12955-12959.	3.1	393
122	Visible light photo-induced antibacterial activity of CNT–doped TiO2 thin films with various CNT contents. Journal of Materials Chemistry, 2010, 20, 7386.	6.7	213
123	Intestinal Parasitic Infections among Inhabitants of Karaj City, Tehran Province, Iran in 2006-2008. Korean Journal of Parasitology, 2009, 47, 265.	1.3	72
124	Storage of Ag nanoparticles in pore-arrays of SU-8 matrix for antibacterial applications. Journal Physics D: Applied Physics, 2009, 42, 135416.	2.8	32
125	Silver nanocube crystals on titanium nitride buffer layer. Journal Physics D: Applied Physics, 2009, 42, 105305.	2.8	18
126	Capping antibacterial Ag nanorods aligned on Ti interlayer by mesoporous TiO2 layer. Surface and Coatings Technology, 2009, 203, 3123-3128.	4.8	71

#	Article	IF	CITATIONS
127	IV vs. IA TPA in Acute Ischemic Stroke with CT Angiographic Evidence of Major Vessel Occlusion: A Feasibility Study. Neurocritical Care, 2009, 11, 76-81.	2.4	26
128	Synthesis and electrochromic study of sol–gel cuprous oxide nanoparticles accumulated on silica thin film. Thin Solid Films, 2009, 517, 6700-6706.	1.8	62
129	Lasting antibacterial activities of Ag–TiO2/Ag/a-TiO2 nanocomposite thin film photocatalysts under solar light irradiation. Journal of Colloid and Interface Science, 2009, 336, 117-124.	9.4	455
130	Physical bounds of metallic nanofingers obtained by mechano-chemical atomic force microscope nanolithography. Applied Surface Science, 2009, 255, 3513-3517.	6.1	7
131	Bactericidal effects of Ag nanoparticles immobilized on surface of SiO2 thin film with high concentration. Current Applied Physics, 2009, 9, 1381-1385.	2.4	131
132	Synthesis of titania/carbon nanotube heterojunction arrays for photoinactivation of E. coli in visible light irradiation. Carbon, 2009, 47, 3280-3287.	10.3	231
133	Photocatalytic property of Fe2O3 nanograin chains coated by TiO2 nanolayer in visible light irradiation. Applied Catalysis A: General, 2009, 369, 77-82.	4.3	143
134	The effect of Au/Ag ratios on surface composition and optical properties of co-sputtered alloy nanoparticles in Au–Ag:SiO2 thin films. Journal of Alloys and Compounds, 2009, 486, 22-28.	5.5	38
135	Hydrothermal synthesis of ZnO nanorod arrays for photocatalytic inactivation of bacteria. Journal Physics D: Applied Physics, 2009, 42, 225305.	2.8	174
136	Enhancement of antibacterial properties of Ag nanorods by electric field. Science and Technology of Advanced Materials, 2009, 10, 015003.	6.1	82
137	Simple Method to Synthesize Na _{<i>x</i>} WO ₃ Nanorods and Nanobelts. Journal of Physical Chemistry C, 2009, 113, 13098-13102.	3.1	26
138	Growth of Na _{0.3} WO ₃ nanorods for the field emission application. Journal Physics D: Applied Physics, 2009, 42, 205405.	2.8	15
139	Photocatalytic Reduction of Graphene Oxide Nanosheets on TiO ₂ Thin Film for Photoinactivation of Bacteria in Solar Light Irradiation. Journal of Physical Chemistry C, 2009, 113, 20214-20220.	3.1	887
140	ZnO Nanowires from Nanopillars: Influence of Growth Time. Current Nanoscience, 2009, 5, 479-484.	1.2	21
141	Self-encapsulation of single-texture CoSi2 nanolayer by TaSi2. Thin Solid Films, 2008, 516, 6008-6012.	1.8	4
142	Growth and characterization of sodium–tungsten oxide nanobelts with U-shape cross section. Journal of Crystal Growth, 2008, 310, 824-828.	1.5	14
143	The effect of Si addition and Ta diffusion barrier on growth and thermal stability of NiSi nanolayer. Microelectronic Engineering, 2008, 85, 548-552.	2.4	0
144	The effect of heating time on growth of NaxWO3 nanowhiskers. Vacuum, 2008, 82, 821-826.	3.5	20

#	Article	IF	CITATIONS
145	Chemical durability of metallic copper nanoparticles in silica thin films synthesized by sol–gel. Journal Physics D: Applied Physics, 2008, 41, 235407.	2.8	21
146	Low temperature self-agglomeration of metallic Ag nanoparticles on silica sol–gel thin films. Journal Physics D: Applied Physics, 2008, 41, 195305.	2.8	38
147	The effect of nanocrystalline tungsten oxide concentration on surface properties of dip-coated hydrophilic WO3–SiO2thin films. Journal Physics D: Applied Physics, 2007, 40, 2089-2095.	2.8	34
148	Hydrophilicity variation of WO3 thin films with annealing temperature. Journal Physics D: Applied Physics, 2007, 40, 1134-1137.	2.8	89
149	rf reactive co-sputtered Au–Ag alloy nanoparticles in SiO2 thin films. Applied Surface Science, 2007, 253, 7438-7442.	6.1	32
150	Thickness dependence on thermal stability of sputtered Ag nanolayer on Ti/Si(100). Applied Surface Science, 2007, 254, 548-551.	6.1	19
151	Formation of gold nanoparticles in heat-treated reactive co-sputtered Au-SiO2 thin films. Applied Surface Science, 2007, 254, 286-290.	6.1	43
152	Effect of Ni, Pd and Ni–Pd nano-islands on morphology and structure of multi-wall carbon nanotubes. Applied Surface Science, 2007, 253, 8458-8462.	6.1	27
153	Physical characteristics of heat-treated nano-silvers dispersed in sol–gel silica matrix. Nanotechnology, 2006, 17, 763-771.	2.6	80
154	Thermal stability of nanoscale silver metallization in Ag/W/Co/Si(100) multilayer. Applied Surface Science, 2006, 252, 5335-5338.	6.1	15
155	Structure transition of single-texture CoSi2 nanolayer grown by refractory-interlayer-mediated epitaxy method. Applied Surface Science, 2006, 253, 2953-2957.	6.1	2
156	Size variation and optical absorption of sol-gel Ag nanoparticles doped SiO2 thin film. Thin Solid Films, 2006, 515, 771-774.	1.8	35
157	An investigation on electrochromic properties of (WO3)1â^'x–(Fe2O3)x thin films. Thin Solid Films, 2006, 515, 644-647.	1.8	23
158	The barrier effect of a WxTa(1â^'x)nanolayer on formation of single-texture CoSi2on Si(1 0 0). Semiconductor Science and Technology, 2006, 21, 1181-1192.	2.0	5
159	Surface modification of exchange-coupled Co/NiOx magnetic bilayer by bias sputtering. Applied Surface Science, 2005, 252, 466-473.	6.1	2
160	Optical properties and surface morphology of evaporated (WO3)1â^'x–(Fe2O3)x thin films. Thin Solid Films, 2005, 484, 124-131.	1.8	52
161	Comment on ÂExperimental realization of a first test of de Broglie–Bohm theoryÂ. Journal of Physics B: Atomic, Molecular and Optical Physics, 2004, 37, 3777-3779.	1.5	3
162	Single-crystalline growth of CoSi2 by refractory-interlayer-mediated epitaxy. Applied Surface Science, 2004, 233, 123-128.	6.1	8

#	Article	IF	CITATIONS
163	The growth of CoSi2 thin film in Co/W/Si(100) multilayer structures. Solid State Communications, 2003, 128, 239-244.	1.9	12
164	Study of cobalt silicides formation in Co/Ta-W/Si(100) multilayer systems. Thin Solid Films, 2003, 433, 298-304.	1.8	6
165	Quantum dense coding by spatial state entanglement. Physics Letters, Section A: General, Atomic and Solid State Physics, 2003, 313, 261-266.	2.1	5
166	A calculation of diffusion parameters for Cu/Ta and Ta/Si interfaces in Cu/Ta/Si(111) structure. Materials Science in Semiconductor Processing, 2003, 6, 165-170.	4.0	25
167	Retardation of Ta silicidation by bias sputtering in Cu/Ta/Si(111) thin films. Journal Physics D: Applied Physics, 2001, 34, 2103-2108.	2.8	29
168	Bias sputtered Ta modified diffusion barrier in Cu/Ta(Vb)/Si(111) structures. Thin Solid Films, 2000, 370, 10-17.	1.8	34